Combining EMD and Lempel-Ziv Complexity for early detection of gear cracks.

M.Kedadouche[1], T.Kidar[1,2], M.Thomas[1] , A.Tahan[1], M. El Badaoui[2] and R. Guilbault[1]

[1]Department of Mechanical Engineering, École de Technologie Supérieure.
1100, Notre-Dame street West, Montreal, H3C 1K3, Quebec, CANADA.
mourad.kedadouche.1@ens.etsmtl.ca; marc.thomas@etsmtl.ca; antoine.tahan@etsmtl.ca; raynald.guilbault@etsmtl.ca
[2]Université de Lyon, Université de Saint Etienne, LASPI EA-3059. 20 Av de Paris, 42334 Roanne Cedex, France.
thameur.kidar@univ-st-etienne.fr; mohamed.elbadaoui@univ-st-etienne.fr

Abstract

Detection of defect and diagnosis of its severity is crucial to avoid catastrophic failures in gearboxes. Vibration analysis is the most used technique for defect monitoring. Early defect detection of gear cracks remains a problem. However, Acoustic Emission (AE) may be used for health monitoring, and diagnosis of rotating machines such as gearboxes. This paper presents the preliminary results of a comparative experimental study using vibration and acoustic emission measurements for monitoring gears crack effects. It appears that, applied to acoustic emission signals, spectrogram allows detection of repetitive shocks generated by rotating defects. This paper investigates two new descriptors based on the combination of Empirical Mode Decomposition and Lempel-Ziv complexity methods. The investigation reveals that the descriptors progressively increase with defect size, and are therefore good candidates for severity diagnosis.

Keywords: Acoustic Emission; Gear, Crack defect, Vibration; Spectrogram; Temporal descriptors; EMD (Empirical Mode Decomposition); Lempel-Ziv Complexity.

1. Introduction

Gearboxes play an important role in industrial applications, and unexpected failures often result in significant economic losses. Typical gear defects include pitting, chipping, and more seriously, tooth cracks. The interest for application of acoustic emission (AE) to condition monitoring in rotating machinery is relatively new, and has grown significantly over the last decade. Mba *and al.* [1] present a review on monitoring gear faults by acoustic emissions. The investigations detailed in [2-6] indicate that AE technique is able to detect bending fatigue degradation, and thus is suitable for vibration monitoring and for early detecting faulty conditions. AE technique may thus be considered as a new condition monitoring tool. Nevertheless, most of these works are limited to time domain conventional methods. On the other hand, numerous papers considering gear condition monitoring through vibration measurements were published over the year. Compared to the classical techniques such as time indicators or Fast Fourier Transform, advanced signal processing techniques like time-frequency analysis (STFT, Wigner-Ville) [7-12] or wavelet transform [13-15] are shown to be more efficient for gear flaw detection. Baydar and Ball proposed the instantaneous power spectrum [16, 17], Wigner–Ville distribution [18] and the wavelet transform method [19] for local tooth fault detection from vibration and acoustic signals. Isa Yesilyurt [20] applied the spectrogram and scalogram approach to gearbox fault detection.

The first part of this paper presents an application of the spectrogram to acoustic signal emissions. A comparison with vibration measurements is conducted; the analysis compares the abilities and effectiveness of the methods for detection of gear flaws. The second part compares the precision obtained from acoustic emission and vibration signals when treated with classical time descriptors. This section also proposes new indicators based on the Empirical Mode Decomposition (EMD) and Complexity approaches.

2. Experimental study

The test rig includes two gear transmission parallel stages. For this investigation, the output gear was artificially damaged with different severity level root cracks. A magnetic brake generates the resistive torque. The tested rotating speeds range from 720 to 2040 rpm. Figure 1 shows the system with the tooth number of each gear.

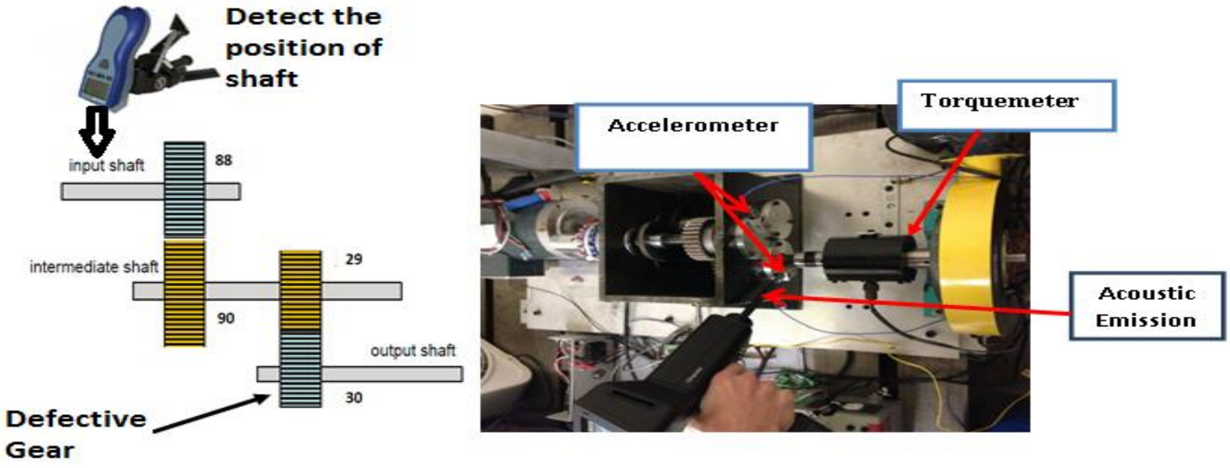

Figure.1 : Test rig.

Figure 2 shows the apparatus used for vibration and acoustic emission measurements. The sensors are an accelerometer (sensitivity of 100 mV/g) and an ultrasound probe (UE Systems UltraProb 10000). Both sensors are connected to an analogue digital converter (THOR Analyzer PRO: DT9837-13310) with a sampling frequency of 48 kHz. The analogue digital converter is connected to a collector-analyzer (BETAVIB). The industrial UltraProb 10000 includes an electrical circuit that converts the original high frequency acoustic emission (AE) signal (detected around a central frequency Fc) into an audible signal AE (0 - 7 kHz). The conversion is based on the heterodyning technique (Fig.2-B). The conversion allows for saving the signal on multiple frequency bands of 7 kHz bandwidth, from 20 kHz to 100 kHz with an increment of 1 kHz. In this study, the central frequency of 30 kHz was used. Artificially cracks (Fig.2-C) of four different sizes were generated for this comparative study. In order to control their size and depth, these cracks were produced with an electric discharge machine. Table 1 gives the crack dimensions.

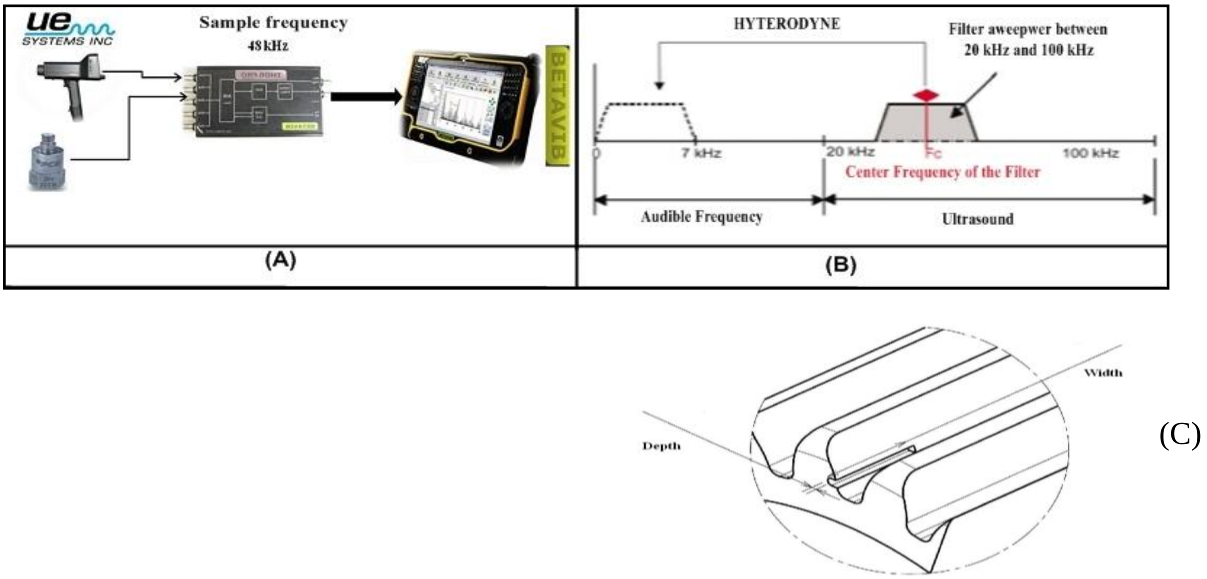

Figure.2 : (A) AE data processing , (B) Heterodyne principle, (C) geometric parameter of the defect.

Table 1 : Artificial tooth cracks

Defect	C1	C2	C3	C4
Depth (%)	13	13	26	39
Width (%)	33	100	100	100

3. Results and analysis

3.1 Acoustic emission for detecting gear cracks

The analysis is made in the angular domain. The time signals are resampled with respect to the tachometric signals. Bonnardot *and al.* in [21] explain the re-sampling methodology. A modal analysis was initially conducted by means of an impact hammer. One gear tooth was struck while a vibro-laser measured the system response (Fig. 3). The results reveal three resonances in the frequency range of interest: 2545, 5090 and 7635 Hz.

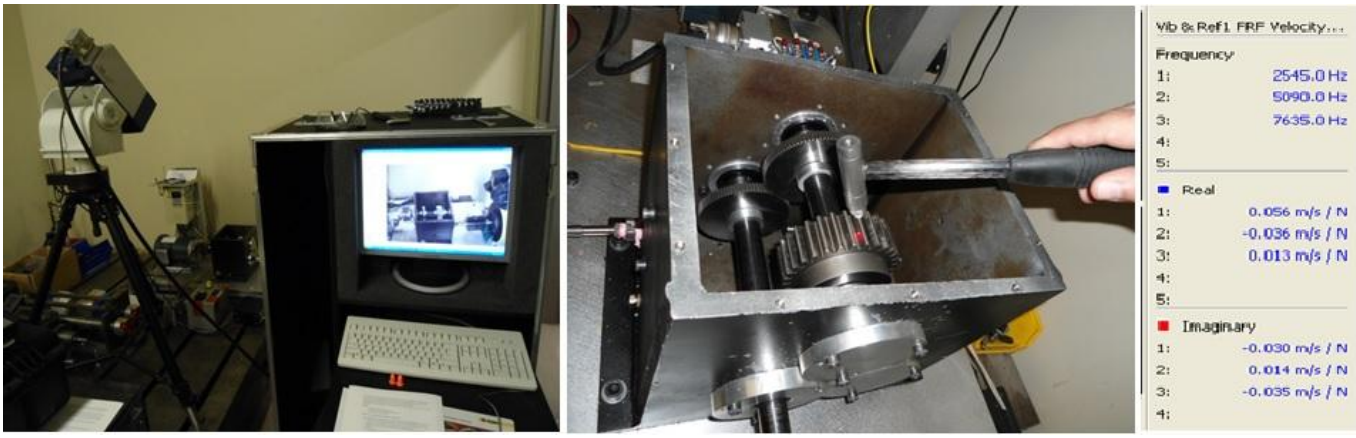

Figure.3: Modal analysis using vibro-laser and impact hammer.

Figure 4 compares the AE spectrum of a gear with a very small defect C1 (blue line) with the AE spectrum of a more damaged gear C2 (red line). Two resonance frequencies clearly appear around 2000 Hz and 5000 Hz, close to the measured resonances. The difference between the light defect and the more defected gear is mainly an energy increase around 2000 Hz. All other damaged gears lead to similar observations; in presence of one crack tooth, acoustic emissions reveal an increase of energy close to the resonance of the gearbox. Figure.5 (A) shows the acoustic emission time signal of gear (C3), while Fig. 5 (B) presents its spectrogram. A repetitive impulse at each revolution of the shaft is clearly visible which excites the first natural frequency.

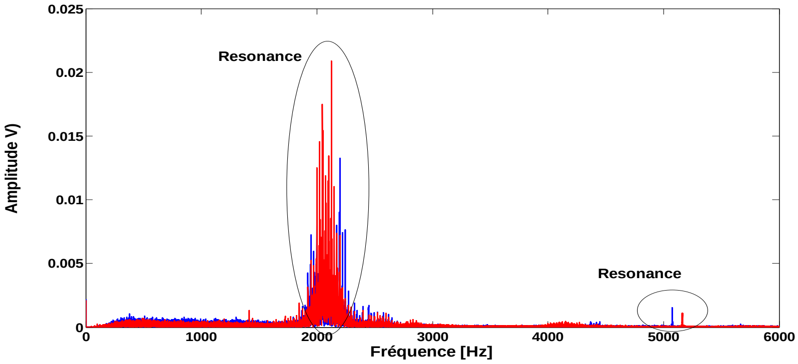

Figure.4: Spectrum of acoustic emission (recorded at 1500 rpm), blue color for the gear with a light defect (C1), red color for a more advanced defect (C2).

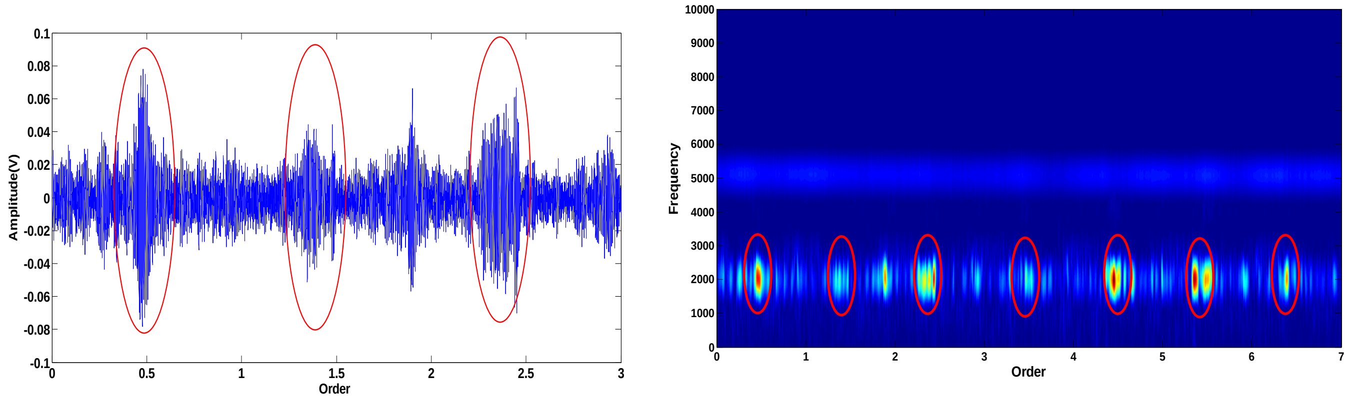

Figure.5: (A) Time signal of defected gear (C3), (B) its spectrogram.

3.2 Comparison between vibration and acoustic emission

Figures 6, 7, 8 and 9 present the spectrogram of acoustic and vibration measurements for the damage gears (level C1, C2, C3 and C4). The test was made at a speed of 720 rpm under a resistive torque of 3 N.m. The AE analysis (Figs 6, 7, 8, 9-A) better show the repetitive impacts produced at each revolution by the defects than the vibration analysis (Figs 6, 7, 8, 9-B). Excepted for case C4, the difference appears even more visible with a defect size increase. With larger root cracks (case C4), the measurements indicate that the defect excites almost all the frequency band (0-9000Hz). This phenomenon can therefore probably serve as a crack size indicator.

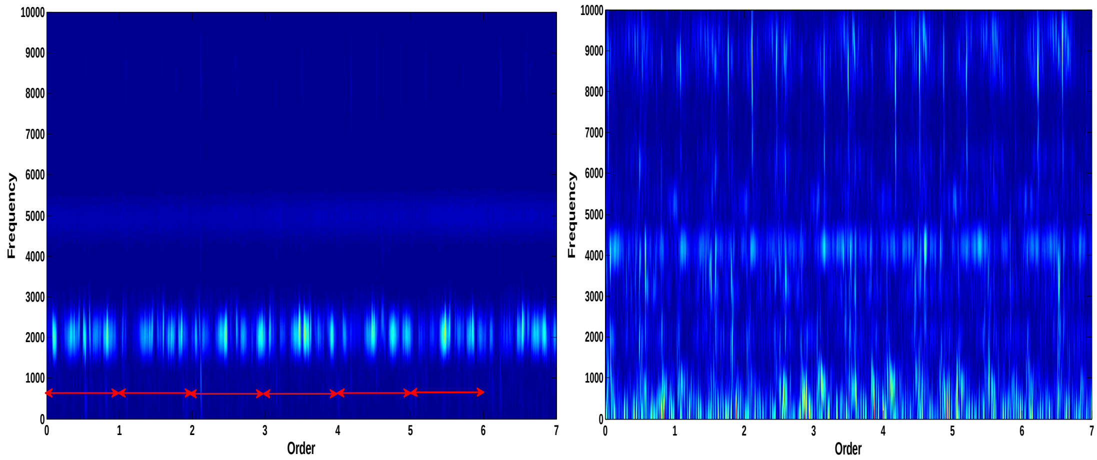

(A) (B)

Figure.6: Spectrogram of defect C1, (A) acoustic emission, (B) Vibration.

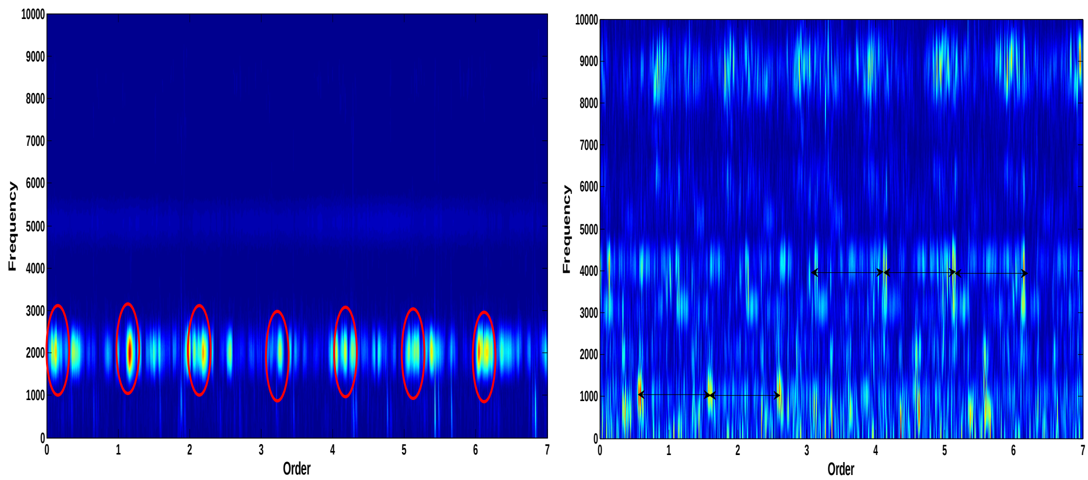

(A) (B)

Figure.7: Spectrogram of defect C2, (A) acoustic emission, (B) Vibration.

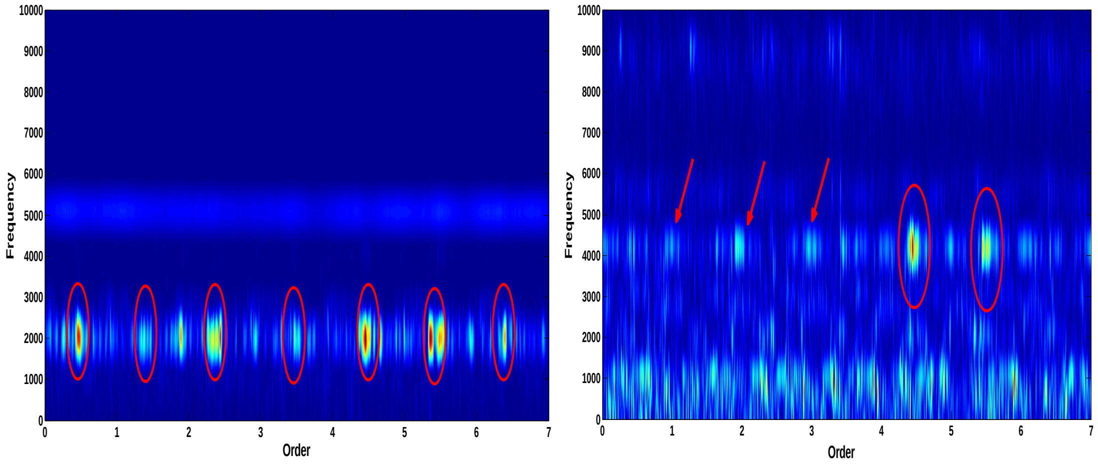

(A) (B)

Figure.8: Spectrogram of defect C3, (A) acoustic emission, (B) Vibration.

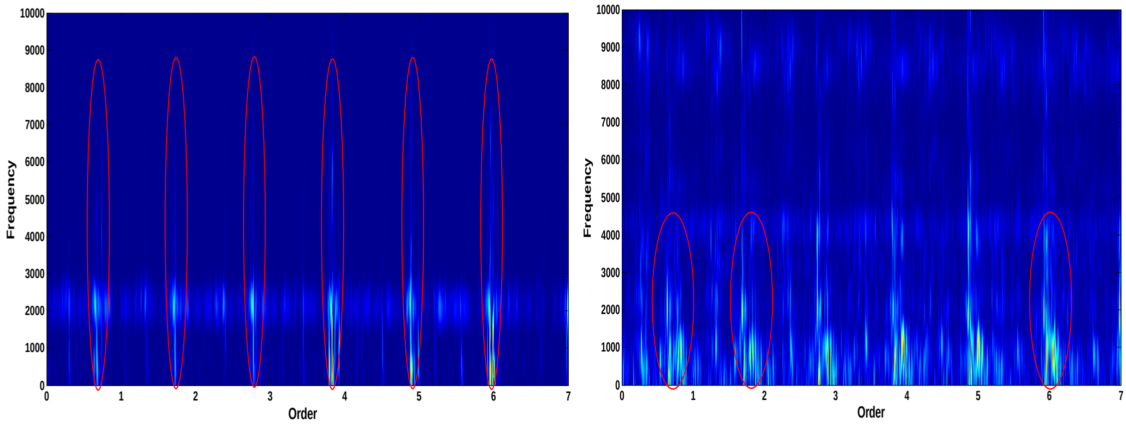

(A) (B)

Figure.9: Spectrogram of defect C4, (A) acoustic emission, (B) Vibration.

3.3 Statistical descriptors

The more popular traditional time statistical descriptors in industry are RMS, Peak and Kurtosis [22]. The following investigate their effectiveness for gear crack detection when applied with AE and vibration measurement. The analysis includes three speeds: 720 rpm, 1500 rpm and 2040 rpm, corresponding to the mesh frequencies listed in Table.2. Figure10 shows the descriptor response when applied to AE signals of increasing root crack size.

Table 2: Mesh frequencies of output gear

Speed (RPM)	fundamental mesh frequency (Hz)	Harmonic1 (Hz)	Harmonic 2 (Hz)	Harmonic 3 (Hz)
720	340.26	680.53	1020.8	1361.11
1500	708.88	1417.8	2126.7	2835.6
2040	964.1	1928.2	2892.3	3856.4

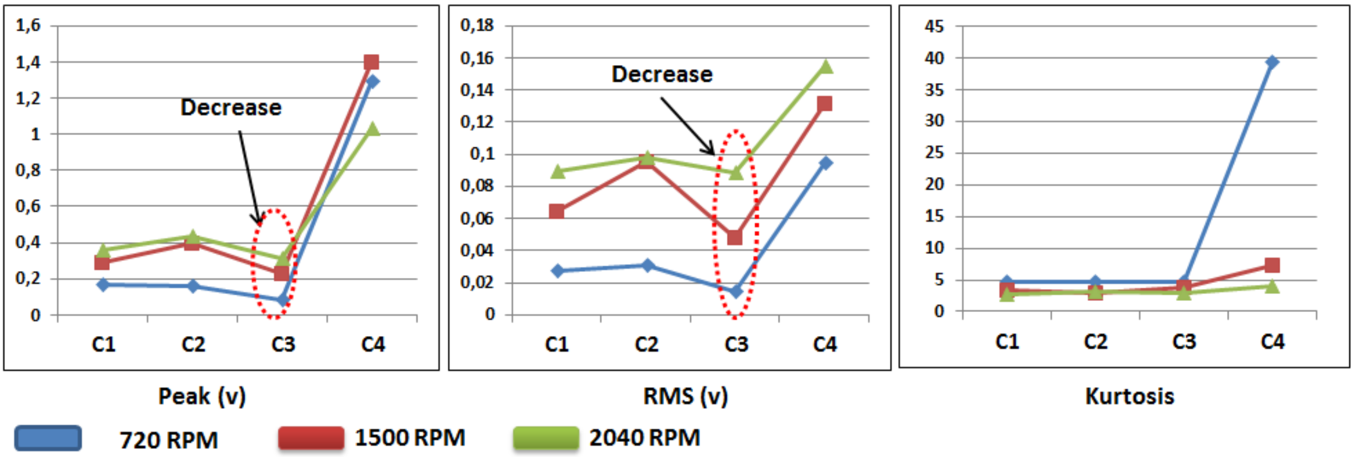

Figure.10: Time indicators: acoustic emission signal.

Figure 10 clearly indicates that the descriptors only detect the larger crack size (case C4). Moreover, Fig. 10 also shows that the descriptor response depends on the rotational speed. Figure.11 presents the same descriptor behaviour when applied to vibration signals. Since the charts of Fig. 11 are similar to those of Fig. 10, the same conclusions may be drawn.

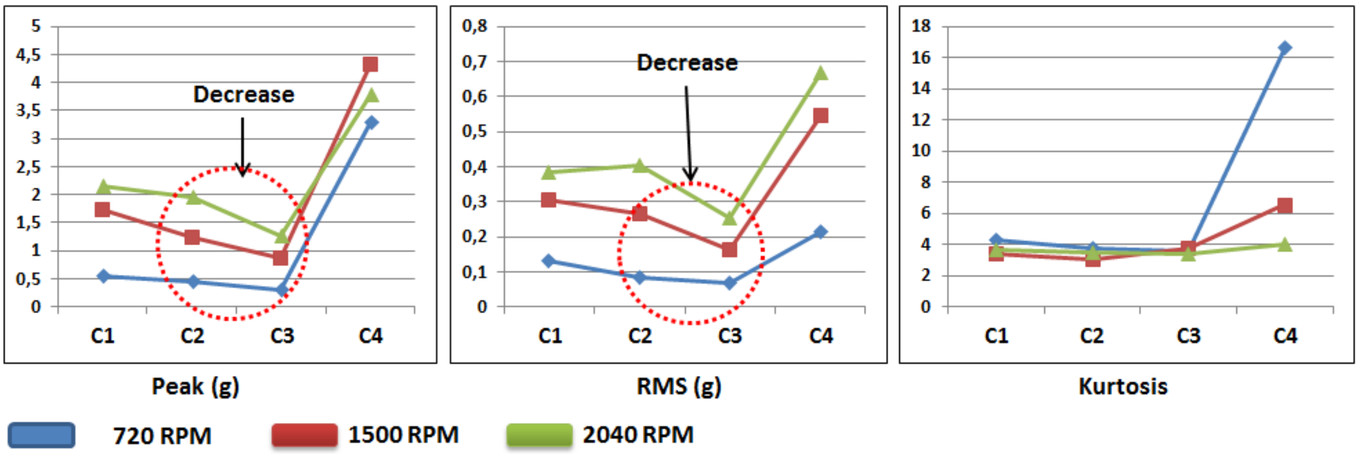

Figure.11: Time indicators: Vibration signal.

4. New indicators based on EMD and Lempel-Ziv complexity

In order to correct the shortcomings revealed in the previous analysis, this section proposes two new indicators. The new formulations are based on the empirical mode decomposition (EMD) method [23-25] and the Lempel-Ziv complexity [26, 27]. They therefore do not consider the energy of the signals, but instead, the distribution of their amplitude and frequency content.

4.1.The Empirical Mode Decomposition (EMD)

EMD proved its efficiency for early defect detection in numerous mechanical systems. Bearing and gear application are good examples [24, 25]. Lei *et al.* [23] presents a good review of EMD applied to fault diagnosis in rotating machinery. EMD decomposes the time signal into a finite set of oscillatory functions called the intrinsic mode functions (*IMF*). An *IMF* function respects the following conditions:

(1) The number of extrema and the number of zero crossings must either equal or differ at most by one;
(2) The value of the moving average envelope defined by local maxima and the envelope defined by local minima are zero.

An intrinsic mode is the embedded time scale in the signal. It corresponds to the mean signal (blue curve in Figure. 12) between two successive extrema (green and red in Fig. 12). An intrinsic mode may include non-stationary amplitudes and modulated frequencies.

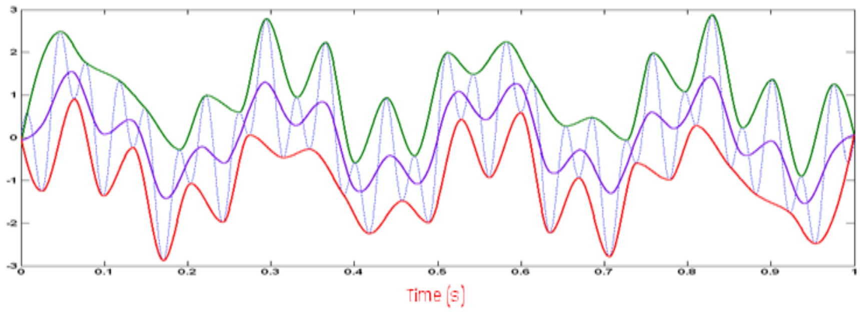

Figure.12 Principle of EMD method

Figure.13 (reproduced from [24]) shows the flow chart of the decomposition method in IMF.

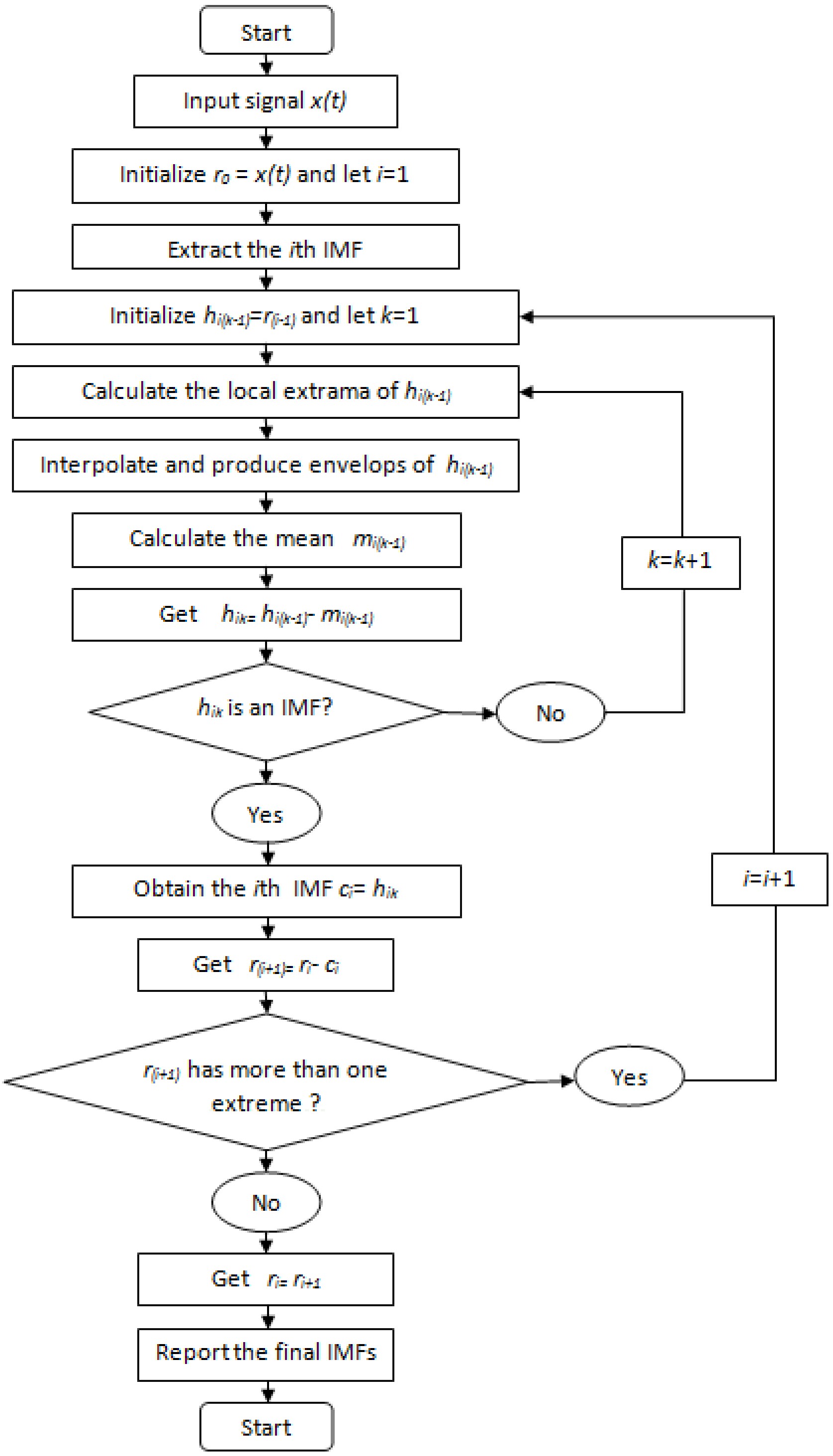

Figure.13 Flow chart of EMD

4.2.Complexity analysis

The complexity analysis is based on the Lempel-Ziv definition [26]. This approach transforms the analysed signal into a data sequence. To illustrate the procedure, consider a gear vibration signal with a known mean value. A new sequence (S) is reconstructed by comparing the value of each sample of the previous sequence within the mean value. If the value of the sample is larger, it is set to one, otherwise to zero. Therefore, only two symbols are present in the new data sequence. This S is subsequently scanned from its first sample to its end. When a subsequence that is not encountered in the previous scanning process is discovered, the complexity value is increased by one. Thus, the Lempel-Ziv complexity reflects the number of all different sub-sequences contained in the original sequence. Figure.14 (reproduced from [27]) described the algorithm. For generality sake, normalized complexity $C(n)$ is often used to obtain a measure independent of the sequence length.

$$C(n) = c(n)/b(n) \tag{1}$$
$$b(n) = n/log2(n) \tag{2}$$

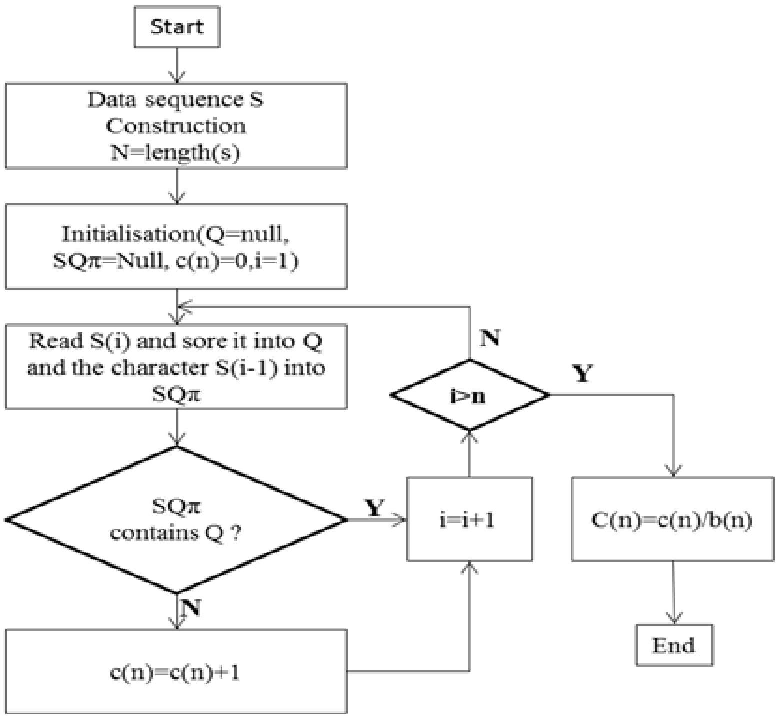

Figure.14: Algorithm of Lempel-Ziv Complexity [27]

4.3.Proposed indicators

- The first indicator is computed from the first Intrinsic Mode Function ($imf_1(n)$) and the residual part $r(n)$of the EMD. The following describes the calculation procedure:
  1. Compute the Lempel-Ziv complexity of original signal $x(n)$, imf_1 and $r(n)$denoted respectively $C(x(n))$, $C(imf_1$ and $C(r(n))$
  2. Compute the Kurtosis of the original signal $x(n)$, imf_1 and $r(n)$denoted respectively $K(x(n)), K(imf_1)$ and $K(r(n))$.
  3. Finally, Eq. 3 gives the indicator 1 formulation:

$$\text{indicator 1} = \left(\frac{C(imf_1) - C(r(n))}{C(x(n))}\right) / \left(\frac{K(imf_1) - K(r(n))}{K(x(n))}\right) \tag{3}$$

- The second indicator is computed from all intrinsic mode functions of the EMD.
  1. Compute the Lempel-Ziv complexity of each imf_i $(i = 1..N)$,
  2. Compute the Kurtosis of the original signal $x(n)$, imf_1 and $r(n)$denoted respectively $K(x(n)), K(imf_1)$ and $K(r(n))$.
  3. Finally, Eq. 4 gives the indicator 2 formulation:

$$\text{indicator 2} = \left(\sum_{i=1}^{N} C(imf_i)\right) \Big/ \left(\frac{K(imf_1) - K(r(n))}{K(x(n))}\right) \tag{4}$$

The two new indicators are applied to AE and vibration signals. The rotational speeds used for the test are 720 rpm, 1500 rpm and 2040 rpm. Figure.15 shows the evolution of the descriptors established for the vibration signals of increasing crack sizes. Both indicators appear to be ineffective.

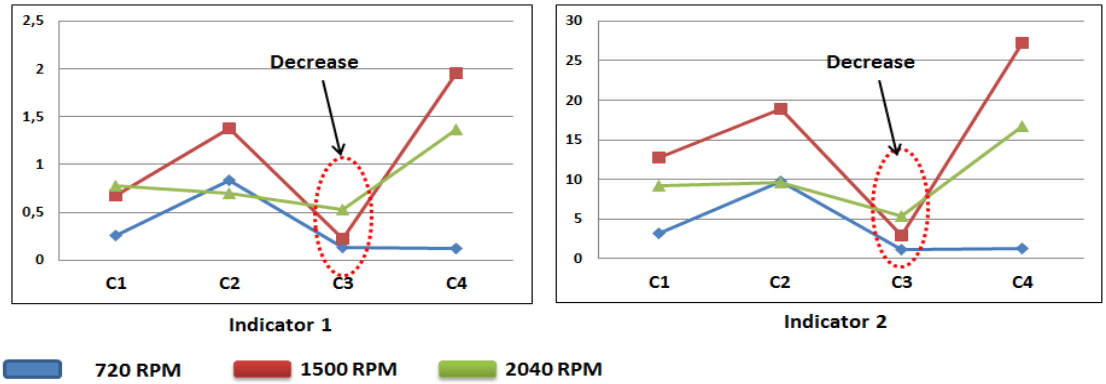

Figure.15: New indicators applied to vibration data.

On the other hand, when applied to AE (Figure.16), both indicators show an amplitude augmentation matching the root crack size increase. Indicator 1 seems also more sensitive. Finally, while visible on the graphs, the rotational speed consequences remain undefined at this stage of the research.

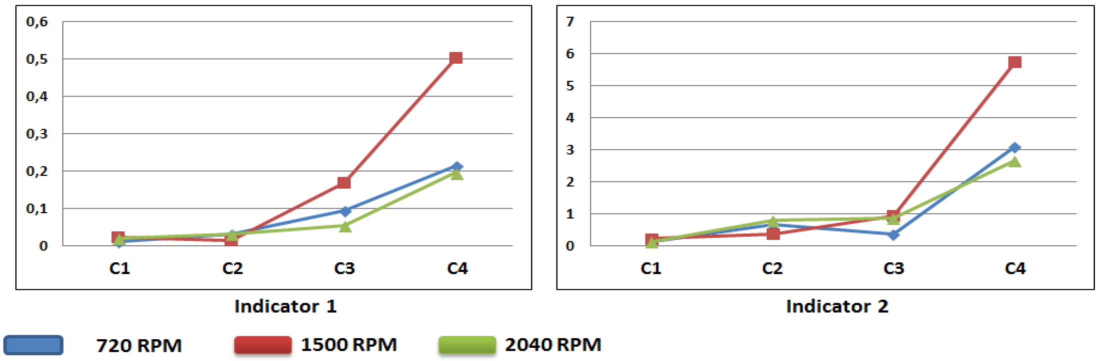

Figure.16: New indicators applied to acoustic emission data.

5. Conclusion

This study investigated the potential of AE for root crack detection in gear systems. The paper compares AE and vibration measurements resulting precisions. The investigation included different root crack sizes and rotation speeds. The first sections indicate that time frequency analysis (spectrogram) assures efficient repetitive shock detection. They also reveal that AE seem more sensitive than vibration measurements. Section 4 of the paper proposes two new indicators. These descriptors are based on EMD and complexity measurement. Both were tested for root crack size monitoring: on the one hand, when applied to vibration signals, the new indicators cannot offer more information than usual time descriptors, while on the other, when applied to AE signals, both appeared to be sensitive to root crack size. They also offered better descriptions than traditional time descriptors. The performance of the new descriptors should be better evaluated in a near future.

Acknowledgments

The financial support of NSERC (Natural Sciences and Engineering Research Council of Canada), FQRNT (Fonds Québecois de la Recherche sur la Nature et les Technologies), MITACS Canada and Pratt & Whitney Canada are gratefully acknowledged.

References

1. M. Mba, D., Rao, Raj B. K. N. Development of Acoustic Emission Technology for Condition Monitoring and Diagnosis of Rotating Machines: Bearings, Pumps, Gearboxes, Engines, and Rotating Structures. The Shock and Vibration Digest, 2006; 38(1), 3-16
2. Miyachika, K., Oda, S. and Koide, T. Acoustic Emission of bending fatigue process of spur gear teeth. Journal of Acoustic Emission. 1995; 13(1/2), S47-S53.
3. Miyachika, K., Zheng, Y., Tsubokura, K., Oda, S., Kanayama, Y., Koide, T., Namba, C. and Hayashi, T. Acoustic Emission of bending fatigue process of super-carburised spur gear teeth. Progress in Acoustic Emission XI. The Japanese Society for NDI. 2002; 304-310.
4. Wheitner, J., Houser, D. and Blazakis, C. Gear tooth bending fatigue crack detection by Acoustic Emissions and tooth compliance. ASME technical paper 93FTM9, 1993; 1-7.
5. Singh, A., Houser, D. R., and Vijayakar, S. Detecting Gear Tooth Breakage Using Acoustic Emission: A Feasibility and Sensor Placement Study. Journal of Mechanical Design. 1999; 121. 587-593
6. T.H. Loutas, G. Sotiriades, I. Kalaitzoglou, V. Kostopoulos. Condition monitoring of a single-stage gearbox with artificially induced gear cracks utilizing on-line vibration and acoustic emission measurements, Applied Acoustics 70 (2009) 1148–1159.
7. Cohen L. Time–frequency distributions—a review. Proc IEEE 1989; 77(7): 941–981.
8. Hlawatsch F and Boudreaux-Bartels GF. Linear and quadratic time–frequency signal representations. IEEE SP Mag 1992; 21–67.
9. Safizadeh M.S., Lakis A.A. and Thomas M., Gear Fault Diagnosis using time-frequency methods, 20th seminar on machinery vibration, CMVA, Quebec, (oct. 2002); 7.19-7.29.
10. Wang WJ and McFadden PD. Early detection of gear failure by vibration analysis –I. Calculation of the time-frequency distribution. MSSP 1993; 7(3): 193–203.
11. Wang WJ and McFadden PD. Early detection of gear failure by vibration analysis –II. Interpretation of the time–frequency distribution using image processing techniques. MSSP 1993; 7(3): 205–15.
12. Safizadeh M.S., Lakis A.A. and Thomas M., Using Short-Time Fourier Transform in Machinery diagnosis, Proceedings of WSEAS (Brazil) 2005, 494-200.
13. Wang WJ, McFadden PD. Application of orthogonal wavelets to early gear damage detection. MSSP 1995; 9(5): 497–507.
14. Wang WJ and McFadden PD. Application of wavelets to gearbox vibration signals for fault detection. JSV 1996; 192(5): 927–39.
15. Safizadeh S., Lakis A. and Thomas M., Machinery Diagnosis by Wavelet Analysis, Proceedings of the 20th international conference of Comadem07, Faro, Portugal, June 2007, 417-424.
16. Baydar N, Ball A. Detection of gear deterioration under varying load conditions by using the instantaneous power spectrum. MSSP 2000; 14(6): 907–21.
17. Baydar N, Chen Q, Ball A, Kruger U. Detection of incipient tooth defect in helical gears using multivariate statistics. MSSP 2001; 15(2): 303–21.
18. Baydar N, Ball A. A comparative study of acoustic and vibration signals in detection of gear failures using Wigner–Ville distribution. MSSP 2001; 15(6): 1091–1107.
19. Baydar N, Ball A. Detection of gear failures via vibration and acoustic signal using wavelet transform. MSSP 2003;17(4): 787–804.
20. Isa Yesilyurt, The application of the conditional moments analysis to gearbox fault detection—a comparative study using the spectrogram and scalogram, NDT&E International 37 (2004) 309–320.
21. F.Bonnardot, M.El Badaoui, R.B.Randall, J. Danière and F.Guillet. Use of the acceleration signal of gearbox in order to perform angular resampling (with limited speed fluctuation). MSSP July 2005, 19(4): 766-785.
22. Sassi S., Badri B. and Thomas M. Tracking surface degradation of ball bearings by means of new time domain scalar descriptors, International Journal of COMADEM, July 2008; ISSN1363-7681, 11 (3), 36-45
23. Lei, Y. G., Lin, J., He, Z. J. and Zuo M. J. : A review on empirical mode decomposition in fault diagnosis of rotating machinery. MSSP, 35(1-2), February 2013; 108-126.
24. M. Kedadouche, M. Thomas and A. Tahan, May 2013. Empirical Mode Decomposition of Acoustic Emission for Early Detection of Bearing Defects. 3rd International Conference on Condition Monitoring of Machinery in Non-Stationary Operations (CMMNO 2013), Ferrara (It), Springer, 11p.
25. Kidar T., M. Thomas, R. Guilbault et M. El Badaoui, 2013. Comparison between the sensitivity of LMD and EMD algorithms for early detection of gear defects. Mechanics & Industry, 14 (2), juin 2013, 121-127.
26. A. Lempel and J. Ziv, “On the complexity of finite sequences,” IEEE Trans. Inform. Theory, Jan. 1976. Vol. IT-22, 75–81.
27. R. Yan and R. Gao. Complexity as a Measure for Machine Health Evaluation, IEEE transactions on instrumentation and measurement, 53 (4), August 2004; 1327-1334.